Journal of the Serbian Chemical Society
JSCS-info@shd.org.rs • www.shd.org.rs/JSCS

J. Serb. Chem. Soc. 85 (4) 531–545 (2020)
JSCS–5320

Original scientific paper

In vitro release study of 2-aminobenzothiazole from microspheres as drug carriers

ASMA MERDOUD[1], MERYEM MOUFFOK[1], ABDERREZZAK MESLI[1]*, NAFA CHAFI[1] and MESSAOUD CHAIB[2]

[1]*Physical and Organic Macromolecular Chemistry Laboratory (LCOPM), Faculty of Exact Sciences, Djillali Liabes University of Sidi Bel-Abbes, Algeria and* [2]*Department of Chemistry, Faculty of Materials Sciences, Ibn Khaldoun University of Tiaret, Algeria*

(Received 26 March, revised 14 November, accepted 18 November 2019)

Abstract: The aim of the present study was the preparation of 2-aminobenzothiazole-loaded microspheres based on cellulose derivatives for controlled and prolonged release. Micro-encapsulation by the simple emulsion (O/W) solvent evaporation method was performed to prepare these formulations using two cellulose derivatives as matrices: ethyl cellulose (EC) and cellulose acetate butyrate (CAB). Optimization of the experimental parameters, such as the polymer/solvent ratio, the matrix type, stirring speed and the number of blades, was performed to obtain a high encapsulation efficiency of the drug. The effect of the selected parameters on microsphere characteristics, as well as the release rate was investigated. SEM images show that the obtained microparticles were spherical in shape. The effective entrapment of 2-amino-benzothiazole (2-ABZT) in the microspheres was confirmed by FTIR spectroscopy and XRD diffraction analysis. The encapsulation efficiency was improved when the polymer concentration increased reaching 89 %. Microspheres in the size range of 61–278 μm with EC and close to 113 μm with CAB were obtained by varying the process conditions. The *in vitro* release kinetics of the cation of 2-ABZT were established at 37 °C in simulated gastric medium pH 1.2 and the obtained data were analyzed according to the Fick law. The results showed that the surface morphology and encapsulation efficiency of the microspheres depended strongly on the polymer/solvent ratio and the release rate could be controlled by adjusting the process conditions.

Keywords: microencapsulation; solvent evaporation method; process parameters; drug release; diffusion.

INTRODUCTION

Antimicrobial drugs have long been used for drug therapy in the field of infectious disease. Many substituted benzothiazole are at the forefront in the

* Corresponding author. E-mail: abderrezzak-mesli@netcourrier.com
https://doi.org/10.2298/JSC190326132M

search for new antimicrobial agents,[1,2] given the isosteric relationship between the SH and NH_2 groups.[3] Recently, a research group was interested in the *in vitro* antifungal activities of synthesized 2-amino-benzothiazole derivatives and showed their novel structure leads to potent antimicrobial activity.[4,5] Previous results proved that an SH moiety at the 2 position of the heterocyclic nucleus significantly increases the antibacterial activity.[4] In addition, 2-ABZT is the amino derivative of the benzothiazole nucleus. This molecule has emerged as a promising active agent against the persistent increase of antimicrobial resistance.[4–6] Benzothiazole is recognized as multitalented scaffold in pharmaceutical chemistry.[7] Thus, benzothiazole derivatives cover a large spectrum of pharmacological activities, such as antimicrobial,[8,9] antidiabetic,[10] antitumor,[11] antitrypanosomal,[12] anticancer,[13] anti-inflammatory and antifungal activity.[6,14] In fact, 2-ABZT acts as a potent inhibitor of lipoxygenase that leads to the blocking of the biosynthesis of leukotrienes B4.[15] Lipoxygenase is an enzyme that catalyzes leukotrienes synthesis and stimulates inflammation and psoriasis.[16] A kinetic study of its hydrolysis from some biological compounds was also reported.[17] Thus, the pH value of the media has a significant effect on 2-ABZT protonation and solubility. Then, the ionization of 2-ABZT in gastric medium promotes the diffusion of a simple ammonium form[18] with a pK_a of 2.51. Hence, its formulation for oral controlled release requires a specific coating able to float over the gastric fluid for a prolonged period.

Various drug forms have been developed to improve the drug pharmacokinetics and effectiveness.[19] Nowadays, polymeric microspheres are considered as the most interesting drug carriers able to achieve controlled release. These systems provide a pH-dependent drug release mechanism.[20–22] In drug microencapsulation,[23–25] the most used class of hydrophobic polymers is cellulose derivatives including ethyl cellulose (EC) and cellulose acetate butyrate (CAB) for a prolonged release.[26] Jelvehgari *et al.* have shown that CAB formulations exhibit enough buoyancy to reside in the stomach over a prolonged and slower drug release.[27]

Initially, in this research, EC and CAB were selected as matrix carriers for the preparation and optimization of microspheres loaded with 2-ABZT. This type of formulations has not been suggested in the literature. In fact, our attention was focused on microspheres as promising drug carriers in the search to enhance the effectiveness of 2-ABZT and more especially, its controlled release. For this purpose, EC and CAB microspheres loaded with 2-ABZT were prepared by microencapsulation using the simple emulsion–solvent evaporation technique.[24] Then, to optimize the experimental formulation parameters, the matrix type, polymer concentration, blade number and stirring speed were varied and their effect on the microspheres size, surface morphology, encapsulation efficiency and the kinetic release profiles investigated.

MATERIALS AND METHOD

Chemicals

2-Aminobenzothiazole (2-ABZT, 99 % purity, Chemical, China), was chosen as a model drug. Ethyl cellulose (EC, viscosity 10 mPa s and cellulose acetate butyrate (CAB) were used as matrix-forming polymers (Sigma–Aldrich, USA). Dichloromethane (DCM, >98 % purity, Fluka). Polyethylene glycol sorbitan monooleate (Tween 80) was purchased from Sigma–Aldrich (USA). For kinetic experiments, simulated gastric solution pH 1.2 was prepared according to the United States Pharmacopeia.[28]

Preparation of cellulose derivatives microspheres

The 2-ABZT loaded microspheres were prepared by the (O/W) emulsion solvent evaporation method.[24] The preparation was realized by varying the parameters, *i.e*., the matrix type (EC or CAB), polymer/solvent ratio (polymer concentration in dichloromethane, 3, 5 and 6 wt. %), stirring speed and blades number (six and four-blade turbine impellers). First, the polymer matrix EC or CAB was dissolved in the organic solvent DCM (32 g), then, the amount of 2-ABZT (0.5 g) was added in this solution with heating under gentle reflux (30 °C) and stirred for homogenization. Simultaneously, the emulsifier Tween 80 was dissolved in 100 g of deionized water (1 wt. %) under heating and mixing. After cooling to room temperature, the internal organic phase was dispersed in the continuous phase in a cylindrical glass reactor (600 mL, ϕ = 80 mm) under constant stirring using a mechanical stirrer (Velp Scientific, ISO 14001, Italy). This emulsion was regularly agitated using four- and six-bladed turbine impellers (blade length = 18 mm for four blades and 12 mm for six blades; blade width = 10 mm) under constant stirring speed (600 and 1200 rpm) for 3 h to harden the oil droplets. Then, the obtained microspheres were recovered by filtration, washed several times with deionized water and vacuum dried in a desiccator in the presence of $CaCl_2$.

Characterization of the microspheres

Determination of the encapsulation efficiency. The amount of encapsulated 2-ABZT in loaded microspheres was determined by dissolving 20 mg of the dried microsphere resin in 20 mL of absolute ethanol in a sealed bottle under constant stirring for 6 h. The resulting solution was analyzed by UV–Vis spectroscopy (Shimadzu UV-2401 PC, Shimadzu, Japan). The actual drug loading (2-ABZT loaded, *DL*, %) and the encapsulation efficiency (*EE*) were calculated according to the following equations:

$$DL = 100(\text{drug mass in microspheres/mass of microspheres}) \quad (1)$$

$$EE = 100(\text{actual drug loading/theoretical drug loading}) \quad (2)$$

Particle size and size distribution. The mean diameter and size distribution (δ) of the microspheres were calculated using optical microscopy (Optika Microscope) and scanning electron microscopy (SEM) by counting more than 500 microspheres using appropriate lenses and the following equations:[29]

$$d_{32} = \sum n_i d_i^{\,3} \Big/ \sum n_i d_i^{\,2} \quad (3)$$

$$d_{10} = \sum n_i d_i \Big/ \sum n_i \quad (4)$$

$$d_{43} = \sum n_i d_i^{\,4} \Big/ \sum n_i d_i^{3} \quad (5)$$

where d_{32} is the mean Sauter diameter; δ the distribution of the microparticulate system calculated as $\delta = d_{43}/d_{10}$; d_{10} is the mean number diameter and d_{43}: the mean weight diameter.

Scanning electron microscopy (SEM). The morphology and surface topography of the microspheres were examined without sputter deposition using a scanning electron microscope (SEM Quanta 200 FEI, Imaging Center–UMS 3420, Bordeaux University, France) at 50 Pas under 12 kV acceleration voltages. The samples of microspheres were deposited on a double--scotched carbon film that was fixed on a stub and observed at different magnifications.

Infrared spectroscopy. The pure 2-ABZT, EC and CAB patterns were compared with those of the microspheres. The FT-IR spectra of the samples in powder form were recorded in the wavenumber range from 400 to 4000 cm^{-1} using an FT-IR spectrometer, equipped with an ALPHA platinum ATR and diamond ATR module (Bruker ALPHA).

XRD spectroscopy. The XRD diffraction patterns were recorded using a Bruker AXS D8 X-ray diffractometer with copper radiation source in the 2θ range from 0 to 60° with a step time of 15 s and a step width of 0.02°. The XRD diffractograms of loaded microspheres, pure 2-ABZT and polymer matrices (EC and CAB) were compared.

In vitro *release studies*

The release studies of the predominate form 2-ABZTH$^+$ in a pH 1.2 medium from microspheres were performed in duplicate using a cylindrical double-wall glass reactor (100 mL). At the time t_0, 100 mg of microspheres was soaked in 100 mL of simulated gastric medium pH 1.2 at 37 °C. The dissolution medium was stirred at 500 rpm for good homogenization. The kinetic study was followed using the sink method: samples of the solution (3 mL) were collected for analysis at determined time intervals and replaced simultaneously by 3 mL of the pH 1.2 medium. The samples were analyzed using UV–Vis spectrophotometer with a cell compartment thermostat at 37 °C (2401PC Shimadzu) at 268 nm.

RESULTS AND DISCUSSION

Characterization of the microspheres

Scanning electron microscopy (SEM) and particle size results. The composition of the prepared microspheres and the process conditions are summarized in Table I. The photomicrographs recorded by the SEM illustrated spherical and individualized microspheres with different aspects. Regarding Fig. 1, a variation of the surface structure was observed when the EC concentration was increased from 3 to 5 and to 6 wt. %, respectively.

TABLE I. Experimental process conditions and encapsulation results of the prepared microspheres; *DL* – drug loading; *EE* – encapsulation efficiency; MS4: formulation prepared using CAB as polymer matrix with the ratio 1:2 of 2-ABZT:polymer**;** MS5: formulation prepared with 4 blades, all the other formulations were prepared with 6 blades; δ – the size distribution

Lot	Matrix	$c_{Polymer}$ wt.%	2-ABZT to polymer ratio	Speed rpm	*DL* / %		*EE* %	d_{32} μm	δ^a
					Theoretical	Actual			
MS1	EC	3	1:2	600	33.33	24	73	166±1.54	1.22±0.19
MS2	EC	5	1:3	600	25.00	20	79	189±1.81	1.30±0.32
MS3	EC	6	1:4	600	20.00	18	89	278±2.77	1.26±0.28
MS4	CAB	3	1:2	600	33.33	27	82	113±0.98	1.19±0.12
MS5	EC	3	1:2	600	33.33	28	84	181±2.33	1.34±0.25
MS6	EC	3	1:2	1200	33.33	18	53	61±0.48	1.10±0.08

A sample of microspheres (MS1) revealed a rough and porous surface structure with a diameter d_{32} of 166 μm (Fig. 1A). For the sample (MS2), microspheres with a wrinkly surface and lower porosity with a diameter of 189 μm were observed (Fig. 1B). Furthermore, the (MS3) microspheres had a tortuous and crumpled surface without any visible pores (Fig. 1C). In fact, the microspheres (MS3) showed a more spherical shape but with a larger Sauter diameter of close to 278 μm. This could be explained by the high percentage of *EC* (6 %), which yielded a high viscosity and so made the rough surface of the microspheres become thicker and wrinkled. Thus, it appears that during the stirring and separation process, both of the polymer matrix and the active principle precipitate resulting in the solidification of loaded-microspheres once the DCM was evaporated, as was shown by Bodmeier and Chen.[30] This parameter strongly affected the surface structure and morphology of the microspheres. In fact, as the EC concentration was increased from 3 to 6 wt. %, the mean Sauter diameter (d_{32}) of the microspheres was significantly increased reaching up to 1.5-fold larger (Table I). Moreover, if the (MS1) and (MS2) batches are compared, the (MS2) had a larger diameter. This is related to the increase in the viscosity of the organic phase, which induced a larger size of emulsion droplets.[31] The achieved particle size distribution values (δ) were lower as the polymer concentration increased, most probably because the resulting particles were stably separated without coalescence of emulsion droplets at higher EC concentrations. In fact, Raut *et al*. in the preparation of metoprolol succinate microspheres mentioned that increased EC or other polymer (such as HPMC) in a fixed volume of solvent increases the viscosity of the medium, which might have diminished the shearing efficiency leading to increased droplet size and hence microsphere size.[41] The same remark was reported for other drug/EC microspheres preparations.[23,41] Considering the nature of the polymer matrix under the same process conditions, The CAB microspheres were smaller than the EC microspheres. Based on the particle sizes values, microspheres with a mean Sauter diameter of 166 μm with EC and of 113 μm with CAB were obtained. Therefore, the investigation of the effect of the number of blades and the stirring speed on the particle size in order to produce the uniform-sized microspheres based on cellulose derivatives was of importance.

According to Table I, the sizes results showed that both increasing the stirring speed and changing the number of blades from four to six yielded smaller microparticles. In fact, when the stirring was increased from 600 to 1200 rpm, the diameter d_{32} of the microspheres was reduced significantly, attaining up to 2.8--fold smaller (Table I). In addition, the particle size distribution values (δ) were similarly decreased as these mechanical forces increased, supporting a more enhanced size-uniformity of the particles. Hence, at higher stirring shear force, which is essential for droplets disruption, the formation of smaller emulsion droplets is easier, resulting in small particle sizes.[32]

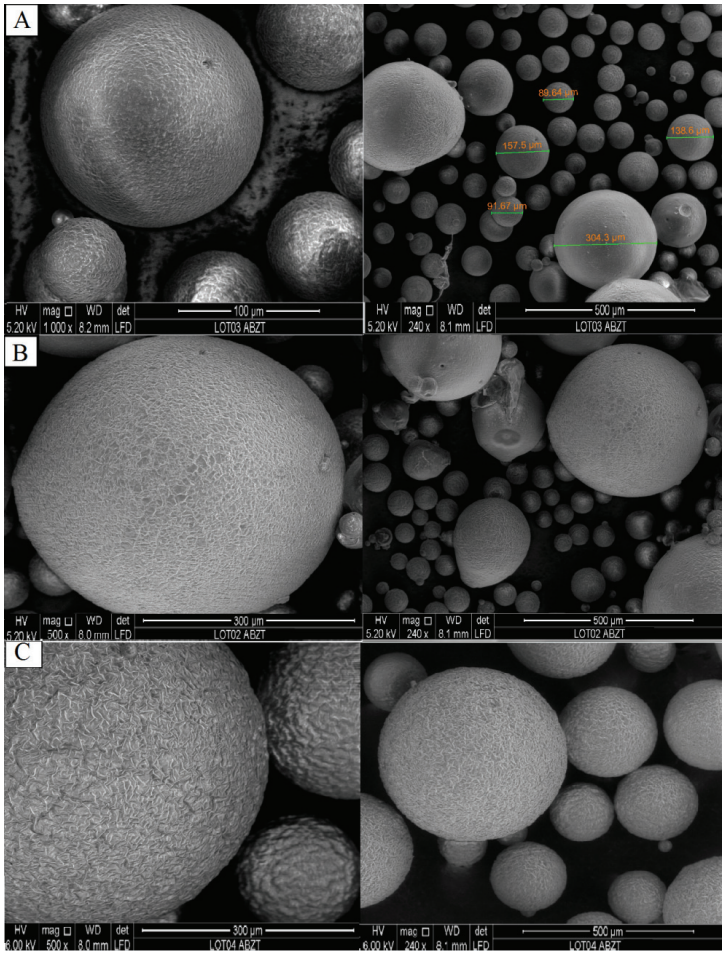

Fig. 1. SEM micrographs of the microspheres prepared at different EC concentrations (A: 3 wt. %, B: 5 wt. % and C: 6 wt. %).

*Drug loading (*DL*) and encapsulation efficiency (*EE*)*

The drug loading, expressed as the percentage of the actual content of 2-ABZT in microspheres to the mass of microspheres, was varied from 18 to 24 % by the changing operative conditions (Table I). It was observed that the drug loading decreased with increasing the EC concentration. Moreover, both increasing the stirring speed and the number of blades had a strong effect on the particle sizes but with lower entrapment efficiency. In fact, the entrapment efficiency was improved practically and exceeded 80 % when a high percentage of polymer (6 wt. %, Table I) was used. This could be explained by the increase in the organic solution viscosity that prevents the diffusion of the entrapped 2-ABZT to the continuous phase during emulsion formation, thereby enhancing its encapsulation.

Considering the matrix type, under the same process conditions, the drug loading was higher in the microspheres prepared with CAB than were those with EC. On increasing the stirring shear force, smaller microspheres were obtained. In addition, the entrapment efficiency gradually decreased in this case, because of the diffusion of 2-ABZT into the aqueous phase caused by the increased turbulence and force.

From Table I, it could be deduced87t that the effects of the selected process parameters on the microspheres sizes, drug loading and encapsulation are well marked.

Infrared spectroscopy

FTIR spectroscopy confirmed the effective presence of 2-ABZT in microspheres (Fig. 2) and identified the chemical stability of the drug.

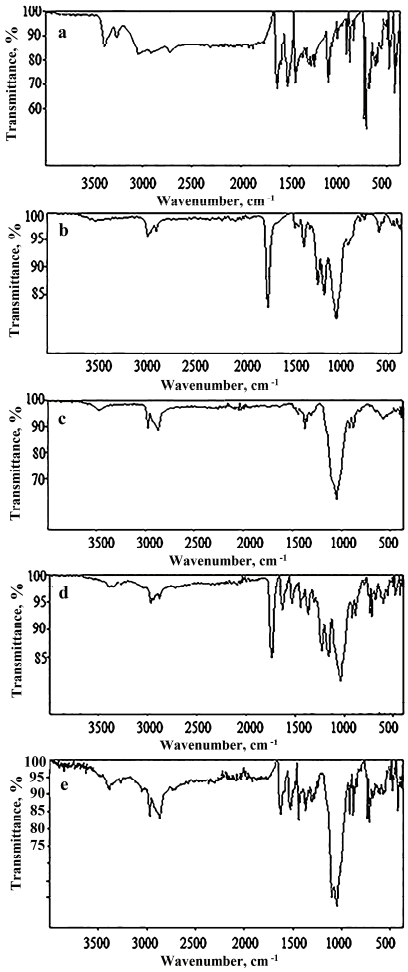

Fig. 2. FT-IR spectra of pure 2-ABZT, matrix (EC and CAB) and loaded microspheres of lots MS1 and MS4 (a: 2-ABZT, b: CAB, c: EC, d: MS4 and e: MS1).

The chemical structures of the drug and polymer matrixes are given in Scheme 1. The FTIR spectra of the 2-ABZT-loaded microspheres were compared with that of pure 2-ABZT and those of the polymer matrices EC and CAB (Fig. 2). Both in IR spectra of EC or CAB microspheres (MS1 and MS4), the specific bands of 2-ABZT appeared clearly at the expected wave number:[33] 3399 and 3274 cm^{-1} for the amine groups (N−H), 1636 cm^{-1} for (C=N) benzothiazole nucleus, 1537 cm^{-1} for aromatic C=C vibration, 1255,37 cm^{-1} bending of (C−S). The IR spectrum of EC showed the O−H stretching band at 3485 cm^{-1}, the stretching vibration of aliphatic C−H band at 2970 and 2870 cm^{-1}, the vibrations of glycosidic band C−O−C at 1070 cm^{-1}. The peak at 1370 cm^{-1} corresponds to the C−O ether functions.[33,34] Then, a series of characteristic absorption peaks for CAB polymer were observed at 2915 and 2879 cm^{-1} (stretching vibration of $–CH_2$), 1747 cm^{-1} (C=O stretching vibration), 1253 and 1429 cm^{-1} (assigned to the symmetric and asymmetric vibrations of –COO) and 1030 cm^{-1} (C–O–C vibration), respectively. Therefore, the IR spectra did not show any new bands and thereby, any chemical interaction between the drug and polymers. Similar to other authors[31–33] and based on this analysis, the incorporation of 2-ABZT did result in any chemical interaction with the polymer matrix.

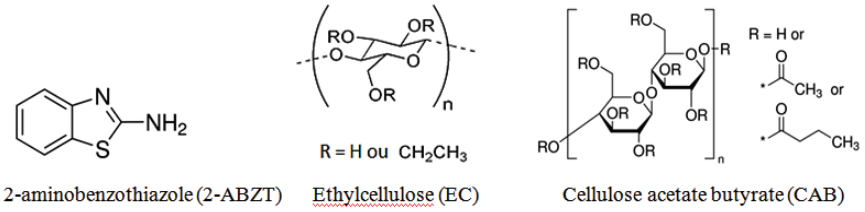

2-aminobenzothiazole (2-ABZT) Ethylcellulose (EC) Cellulose acetate butyrate (CAB)

Scheme 1. Chemical structures of the used materials.

XRD spectroscopy

The XRD diffraction technique was utilized to analyze the crystal structure of the drug entrapped in the microspheres. The crystalline nature of the encapsulated 2-ABZT was clearly proved by the characteristics of the XRD pattern, containing well-defined peaks with a high intensity at 11.5, 14, 16, 18.2, 20.9, 22.2, 23.2, 24.5, 27, 28.5, 29.2, 32.7, 34, 35.2, 37.2 and 40.5° within the 2θ range from 5 to 70° (Fig. 3). Moreover, the X-ray diffractograms of EC and CAB indicated the amorphous state of the polymer matrix. Only one sharp peak at a 2θ value of 11° was observed in the EC diffractogram, indicating a very small crystalline zone, as remarked by Trivedi *et al.*[34] However, the XRD analysis of the 2-ABZT-loaded cellulose derivative microspheres exhibited some characteristic diffraction patterns appropriated to 2-ABZT that were less intense as compared to those of pure 2-ABZT.

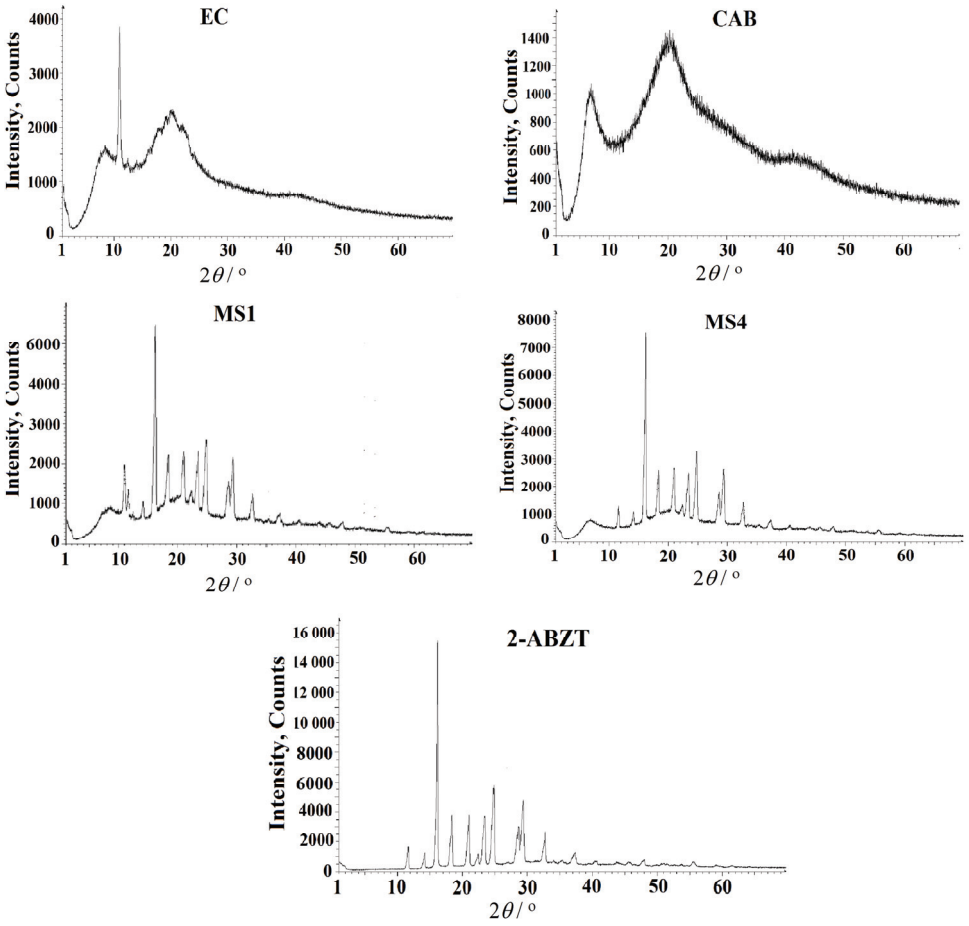

Fig. 3. XRD Diffraction patterns of pure 2-ABZT, cellulose derivatives (EC and CAB) and the loaded microspheres MS1 and MS4.

The results showed clearly the diminution of the crystalline nature of 2-ABZT when it was encapsulated in these microspheres. Actually, it could be observed that the peak intensity in the XRD diffraction patterns decreased significantly when the active agent was microencapsulated in the microspheres, indicating that it was entrapped in the crystalline form. However, there was no shifting of any characteristic peaks after drug encapsulation. Practically, the same absorption bands appeared in the microspheres spectrum after drug encapsulation. It is difficult to imagine that a chemical reaction between 2-ABZT and the polymer matrix could occur at room temperature during the encapsulation process, only chemical interactions, such as hydrogen bonding, *etc*., could be formed. Thus, the

results of the XRD analysis confirmed the FTIR results that there were chemical interactions between the drug and the polymer matrix.

In vitro *release study*

With the objective of testing and studying the controlled release formulations, the *in vitro* release kinetics of 2-ABZTH$^+$ were performed in simulated gastric fluid at pH 1.2 (SGF, hydrochloric acid solution) at 37 °C for all the microspheres. The profiles of the 2-ABZTH$^+$ released from microspheres as a function of time are shown in Fig. 4. The results indicated that the percentage of EC used had a significant effect on the 2-ABZTH$^+$ release from the microspheres. From Fig. 4, it could be seen that the release rate of 2-ABZTH$^+$ was gradually delayed as the EC concentration increased from 3 to 5 wt. % and to 6 wt. %. For the MS1 microspheres, the 2-ABZTH$^+$ was rapidly discharged, a notion that was supported by SEM analysis since these microspheres showed a porous surface (Fig. 1A) that contributed to a rapid release rate. Alternatively, the release is likely to be governed by diffusion inside opened pores and percolation channels, when the porosity of the microspheres increased, the percentage of 2-ABZTH$^+$ released also increased.

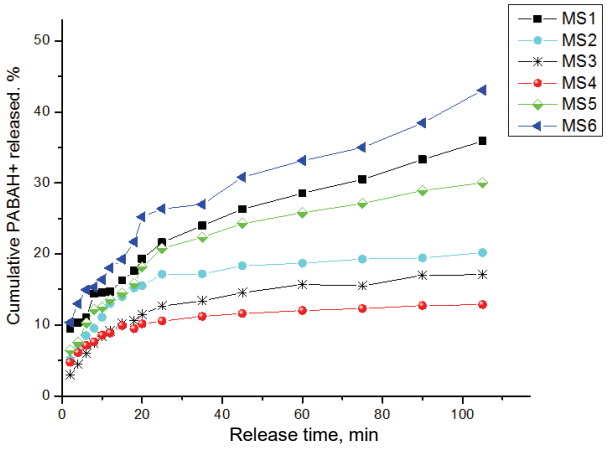

Fig. 4. Release profiles of 2-ABZTH$^+$ from microspheres MS1–MS6 in pH 1.2 at 37 °C.

Hence, during emulsion formation, the solidification of microspheres was faster at higher EC concentrations, which results in a viscous polymer layer at the emulsion droplets within the formation of a rougher surface. It seems that increasing the polymer concentration made the gel more swollen become denser and by this mean reducing the release rate. On comparing the two matrices, the CAB polymer exhibited a slower release rate. In fact, the results demonstrated that 2-ABZTH$^+$ was quickly released from the microspheres MS1 and MS6. However, if MS1 and MS6 are compared, the microspheres MS1 exhibited a slow rel-

ease, whilst it was higher from microspheres MS6. In addition, the same trend was found during all release times with a noticeable increase in the release as the stirring speed level and the blades number increased. This is certainly related to the size of these two microspheres batches (MS1 and MS6). Thus, the results appear to be coherent since the size of these microspheres was smaller, which then led to a greater surface contact of the microspheres with the release medium, and thereby a rapid release rate is favored.[35–37] By plotting the two repeated kinetics for a single batch, the values obtained are close and therefore the two graphs are identical.

Data release mechanisms and mathematical analysis

The mathematical description of drug diffusion is frequently based on the Fick second law in order to evaluate the release kinetics.[38] Many theoretical or empirical models were used with the objective of explaining the process of drug release. This process is correlated with mass transfer controlled by diffusion. In this study, the obtained release data were analyzed using the kinetic models of Higuchi[39] and Ritger–Peppas[40] for quantitative prediction of the controlled drug release. Thus, the choice of the best model is based on the higher correlation coefficient value (r^2). Higuchi explained drug release from a matrix system by a simple relationship:

$$Q_t = k_H t^{1/2} \quad (6)$$

where, Q_t is the amount of 2-ABZTH$^+$ released as a function of time and k_H is the Higuchi dissolution constant. Furthermore, to confirm the mechanism of drug release, Ritger and Peppas elucidate the following equation:

$$M_t/M_\infty = k_{RP} t^n \quad (7)$$

where the ratio M_t/M_∞ represent the fraction of the 2-ABZTH$^+$ released at time t, M_t: (2-ABZTH$^+$)$_t$ and M_∞: (2-ABZTH$^+$)$_\infty$, the amounts of 2-ABZTH$^+$ released at time t and time ∞, respectively, and k_{RP} is the Ritger–Peppas release constant and n represent exponent which characterizes the drug release mechanism. The interpretation of n values was realized in the following manner: n ≤shows Fickian diffusion (Case I); $0.5 \leq n \leq 1$ corresponds to a non-Fickian mechanism: Anomalous (erosion and diffusion) release; $n = 1$ indicates Case II transport (zero order) and $n \geq 0.89$ designates super-Case II release (relaxation). The Higuchi model showed good linear fits confirming that the release of 2 ABZTH+ is, generally, governed by the diffusion mechanism (Fig. 5).

Based on the r^2 values of the correlation coefficient, the most suitable kinetic model describing the release mechanism of 2-ABZTH$^+$ is the Higuchi model with a higher correlation coefficient r^2 of more than 0.96. In fact, the drug release depends on selected parameters. The results of the Higuchi's model indicated that

the release constant (k_H) varied from 1.011 to 2.810 $min^{-1/2}$ (Table II). Data analysis according to the Higuchi model confirmed the rapid release of 2-ABZTH$^+$ from the microspheres MS6, where the value of the release constant k_H was higher.

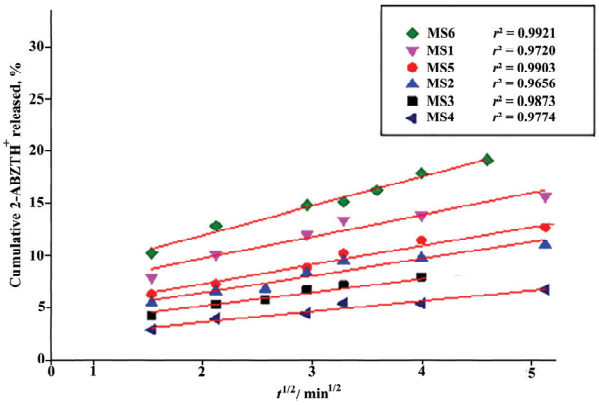

Fig. 5. Higuchi plot of the percentage 2-ABZTH$^+$ released from microspheres MS1–MS6 as a function of the square root of time.

TABLE II. Data analysis results of 2-ABZTH$^+$ release; k_H and k_{RP} – the release constants for Higuchi and Ritger–Peppas, respectively; n – the release exponent; r^2 – the correlation coefficient

Code	Matrix	Higuchi model		Ritger–Peppas model		
		k_H / $min^{-1/2}$	r^2	n	k_{R-P} / min^{-n}	r^2
MS1	EC	1.311	0.9873	0.43	0.0827	0.9988
MS2	EC	1.103	0.9903	0.45	0.0691	0.9975
MS3	EC	1.037	0.9656	0.41	0.0442	0.9948
MS4	CAB	1.011	0.9774	0.57	0.0078	0.9932
MS5	EC	2.090	0.9720	0.39	0.0336	0.9881
MS6	EC	2.810	0.9921	0.41	0.0488	0.9937

The comparison between the formulations MS1, MS2 and MS3 showed that the microspheres MS3 discharged the 2-ABZTH$^+$ with a low release constant k_H. This result is certainly due to both the high polymer concentration and the sizes of the microspheres. For the microspheres MS1, the presence of pores at the surface of microspheres as observed in the SEM micrographs allows a rapid and easy penetration of the solution pH 1.2 and then the 2-ABZTH$^+$ dissolution and release. In order to characterize the mechanism of drug release, the Ritger–Peppas equation was applied and the value of the exponent n was calculated (Table II). Based on the n value that ranged from 0.39 to 0.57, it was concluded that for all microspheres except formulation MS4, the 2-ABZTH$^+$ release was governed by diffusion, according to the Fickian mechanism since $n \leq 0.45$, in this case, the 2-ABZTH$^+$ diffused out of the microspheres through the hydrophobic matrix *via*

the water-filled pores. For the MS4 formulation based on a CAB matrix, the value of n was higher than 0.45 and, in this case, the dissolution mechanism is governed by a non-Fickian mechanism.

CONCLUSIONS

The present study was directed to the preparation of 2-ABZT controlled release microspheres based on cellulose derivatives as matrices. The optimization of the experimental parameters of the microencapsulation by adjusting some conditions allowed the determination of the favored parameters to develop spherical and individualized microspheres with high encapsulation efficiency. SEM micrographs showed microspheres with different surface morphology and the mean Sauter diameter d_{32} of microspheres ranged from 61 to 278 μm. In fact, smaller and spherical microspheres were obtained when the stirring speed was increased. Moreover, the CAB microspheres were smaller than the EC ones. The results showed that the surface morphology and the encapsulation efficiency of the microspheres depended strongly on the polymer concentration. The drug entrapment was especially related to the initial drug/polymer ratio in the microspheres. The particle size could be controlled practically by the stirring speed during emulsion and the polymer concentration. Hence, these factors play crucial roles in the design of the microspherical system. Beside the *in vitro* release study in a complementary work, *in vivo* tests will be required in future studies to evaluate the therapeutic activity of the 2-ABZT.

ИЗВОД

In vitro КОНТРОЛИСАНО ОТПУШТАЊЕ 2-АМИНОБЕНЗТРИАЗОЛА ИЗ ПОЛИМЕРНИХ МИКРОСФЕРА

ASMA MERDOUD[1], MERYEM MOUFFOK[1], ABDERREZZAK MESLI[1], NAFA CHAFI[1] и MESSAOUD CHAIB[2]

[1]*Physical and Organic Macromolecular Chemistry Laboratory (LCOPM), Faculty of Exact Sciences, Djillali Liabes University of Sidi Bel-Abbes, Algeria* и [2]*Department of Chemistry, Faculty of Materials Sciences, Ibn Khaldoun University of Tiaret, Algeria*

У оквиру овог рада приказана је израда микросфера на бази деривата целулозе са инкапсулираним леком, 2-аминобензтриазолом (2-ABZT), за његово контролисано и придужено отпуштање. За микроинкапсулацију лека коришћен је поступак отпаравања лако испарљивог растварача из емилзије (уље/вода). Етил-целулоза (EC) и ацетат–бутират целулозе (CAB) су коришћене као полимерне матрице. Процесни параметри израде миксосфера су оптимизовани варирањем односа полимер/растварач, типа полимерне матрице, брзине мешања и броја лопатица пропелера како би се постигла висока ефикасност инкапсулације лека. Изучаван је утицај изабраних процесних параметара на карактеристике микросфера као и на брзину ослобађања лека из полимерне матрице. SEM анализа је показала да су добијене микрочестице сферног облика. Успешност инкапсулације 2-ABZT у микросфере је потврђена FTIR спектроскопијом и XRD дифракцијом. Ефикасност инкапсулације лека се побољшавала са повећањем концентрације полимера у емулзији, достижући 89 %. Величина микросфера на бази EC се била у опсегу од 61–278 μm у зависности од процесних параметара, док је за CAB микросфере износила око 113 μm. Кинетика отпуштања лека 2-ABZT у катјонском облику је праћена

in vitro, у симулираном желудачном медијуму на pH 1,2 и 37 °C, а добијени подаци су анализирани користећи Фиков закон дифузије. Установљено је да морфологија микросфера и ефикасност инкапсулације лека зависе од односа полимер/растварач, као и да се брзина отпуштања лека из микросфера може контролисати подешавањем процесних параметара.

(Примљено 26. марта, ревидирано 14. новембра, прихваћено 18. новембра 2019)

REFERENCES

1. S. L. Khokra, K. Arora, H. Mehta, A. Aggarwal, M. M. Yadav, *Int. J. Pharm. Sci. Res.* **2** (2011) 1356 (http://dx.doi.org/10.13040/IJPSR.0975-8232.2(6).1356-77)
2. R. V. Patel, P. K. Patel, P. Kumari, D. P. Rajani, K. H. Chikhalia, *J. Med. Chem.* **53** (2012) 41 (http://dx.doi: 10.1016/j.ejmech.2012.03.033)
3. D. Armenise, M. Muraglia, M. A. Florio, N. De Laurentis, A. Rosato, A. Carrieri, F. Corbo, C. Franchini, *Arch. Pharm. Chem. Life Sci.* **345** (2012) 407 (https://doi.org/10.1002/ardp.201100309)
4. A. Catalano, A. Carocci, I. Defrenza, M. Muraglia, A. Carrieri, F. Van Bambeke, A. Rosato, F. Corbo,C.Franchini, *Eur. J. Med. Chem.* **64** (2013) 357 (https://doi.org/10.1016/j.ejmech.2013.03.064)
5. M. N. Bhoi, M. A. Borad, N. K. Panchal, H. D. Patel, *Int. Lett. Chem. Phys. Astron.* **53** (2015) 106 https://doi.org/10.18052/www.scipress.com/ILCPA.53.114)
6. M. N. Bhoi, M. A. Borad, H. D. Patel, *Synth Com.* **44** (2014) 2427 (https://doi.org/10.1080/00397911.2014.907426)
7. A. Gupta, *Asian J. Pharm. Pharmacol.* **4** (2018) 522 (https://doi.org/10.31024/ajpp.2018.4.4.21)
8. B. Rajeeva, N. Srinivasulu, S. M. Shantakumar, *J. Chem.* **6** (2009) 775 (https://doi.org/10.1155/2009/404596)
9. B. L. Eun, K. K. Soon, G. K. Sang, *Arch. Pharm. Res.* **22** (1999) 44 (https://doi.org/10.1007/BF02976434)
10. X. Su, N. Vicker, D. Ganeshapillai, A. Smith, A. Purohit, M. J. Reed, B. V. L. Potter, *Mol. Cell.Endocrinol*. **248** (2006) 214 (http://dx.doi.org/10.1016/j.mce.2005.10.022)
11. T. Bradshaw, A. Westwell, *Curr. Med. Chem.* **11** (2004) 1009 (https://doi.org/10.2174/0929867043455530)
12. J. Neres, M. L. Brewer, L. Ratier, H. Botti, A. Buschiazzo, P. N. Edwards, P. N. Mortenson, M. H. Charlton, P. M. Alzari, A. C. Frasch, R. A. Bryce, K. T. Douglas, *Bioorg. Med. Chem. Lett.* **19** (2009) 589 (https://doi.org/10.1016/j.bmcl.2008.12.065)
13. R. S. Keri, M. R. Patil, S. A. Patil, S. Budagumpi, *Eur. J. Med. Chem*. **89** (2015) 207 (https://doi.org/10.1016/j.ejmech.2014.10.059)
14. P. Venkatesh, N. S. Pandeya, *Inter. J. Chem. Tech. Res.* **1** (2009) 1354 (https://www.researchgate.net/publication/242656820)
15. D. Hadjipavlou-Litina, A. Geronikaki, *Drug Des. Discov*. **15** (1998) 199 (https://europepmc.org/article/med/9689502)
16. K. Muller, *Arch. Pharm*. **327** (1994) 3 (https://doi.org/10.1002/ardp.19943270103)
17. F. Benachenhou, N. Mimouni, Y. Mederbel, R. Kaid Slimane, *Arab. J. Chem.* **5** (2012) 245 (https://doi.org/10.1016/j.arabjc.2010.10.022)
18. F. Tay, M. Duran, S. Demiraya, *Indian J. Chem*. **52** (2014) 102 (http://nopr.niscair.res.in/handle/123456789/25325)
19. J. Alcorn, P. J. McNamara, *Adv. Drug Deliv. Rev.* **55** (2003) 667 (https://doi.org/10.1016/S0169409X(03)000309)

20. J. Vysloužil, P. Doležel, M. Kejdušová, E. Mašková, J. Mašek, R. Lukáč, V. Košťál, D. Vetchý, K. Dvořáčková , *Acta Pharm.* **64** (2014) 403 (https://doi.org/10.2478/acph-2014-0032)
21. S. Chirani, M. O. Lebig, S. Bouameur, M. Mouffok, N. Chirani, N. Chafi, K. Guemra, *Indian J. Pharm. Educ.* **51** (2017) 79 (https://doi.org/10.5530/ijper.51.2s.53)
22. B. Tyler, D. Gullotti, A. Mangraviti, T. Utsuki, H. Brem, *Adv. Drug Deliv. Rev*. **107** (2016) 163 (https://doi.org/10.1016/j.addr.2016.06.018)
23. Z. El Bahri, J.-L. Taverdet, *J. Appl. Polym. Sci.* **103** (2007) 2742 (https://doi.org/10.1002/app.25488)
24. G. Subedi, A.K. Shrestha, S. Shakya, *Open Pharm. Sci. J*. **3** (2016) 182 (https://doi.org/10.2174/1874844901603010182)
25. Y. Li, H. He, *Asian J. Pharm. Sci.* **11** (2016) 771 (https://doi.org/10.1016/j.ajps.2016.07.004)
26. G. Murtaza, *Acta. Pol. Pharm. Drug Res.* **69** (2012) 11 (https://www.researchgate.net/publication/224937816)
27. M. Jelvehgari, M. Maghsoodi, H. Nemati, *Res. Pharm. Sci.* **5** (2010) 29 (https://www.researchgate.net/publication/51143951)
28. United States Pharmacopeia (USP 27), *The National Formulary (NF 22)*, 2004 (ISBN 9781889788197)
29. K. Kaczmarski, J. C. Bellot, *Acta Chromatogr.* **13** (2003) 22 (https://www.researchgate.net/publication/237326465)
30. R. Bodmeier, H. Chen, *J. Control. Rel*. **10** (1989) 167 (https://doi.org/10.1016/01683659(89)90059-X)
31. M. Iqbal, N. Zafar, H. Fessi, A. Elaissari, *Inter. J. Pharm*. **496** (2015) 173 (https://doi.org/10.1016/j.ijpharm.2015.10.057)
32. Z. Urbán-Morlán, S. E. Mendoza-Elvira, R. S. Hernández-Cerón, S. Alcalá–Alcalá, H. Ramírez –Mendoza, A. Ciprián-Carrasco, E. Piñón-Segundo, D. Quintanar-Guerrero, *J. Mex. Chem. Soc*. **59** (2015) 173 (https://doi.org/10.29356/jmcs.v59i3.32)
33. R. M. Silverstein, G. C. Bassler, T. C. Morill, *Spectrometric Identification of Organic Compounds*, 4th ed., Wiley, New York, 1981 (ISBN 9780471029908)
34. M. K. Trivedi, A. Branton, D. Trivedi, G. Nayak, R. K. Mishra, *Inter. J. Biomed. Mater. Res.* **3** (2015) 83 (https://doi.org/10.11648/j.ijbmr.20150306.12)
35. M. Mouffok, A. Mesli, I. Abdelmalek, E. Gontier, *J. Serb. Chem. Soc.* **81** (2016) 118 (https://doi.org/10.2298/JSC160308068M)
36. O. C. Larbi, H. Merine, Y. Ramli, F. Benali Toumi, K. Guemra, A. Dehbi, *J. Serb. Chem. Soc.* **83** (2018) 1243(https://doi.org/10.2298/JSC171112065L)
37. N. Assas, Z. Elbahri, M. Baitiche, F. Djerboua, *Asia-Pac. J. Chem. Eng.* **14** (2019) 1 (https://doi.org/10.1002/apj.2283)
38. J. Cranck, *The mathematics of diffusion*, 2nd ed., Clarendon, Oxford, 1976, 85 (ISBN 0 19 853344 6)
39. T. Higuchi, *J. Pharm. Sci*. **52** (1963) 1145 (https://doi.org/10.1002/jps.2600521210)
40. P. L. Ritger, N. A. Peppas, *J. Control. Rel.* **5** (1987) 37 (https://doi.org/10.1016/01683659(87)90035-6)
41. N. S. Raut, S. Somvanshi, A. B. Jumde, H. M. Khandelwal, M. J. Umekar, N. R. Kotagale, *Int. J. Pharm. Investig.* **3** (2013) 163 (https://doi.org/10.4103/2230-973X.119235)
42. M. Sharma, S. Kohli, A. Dinda, *Saudi Pharm. J*. **23** (2015) 675 (https://doi.org/10.1016/j.jsps.2015.02.013).